Numerical simulation of the defect density influence on the steady state response of a silicon-based p–i–n cell

2004 J. Phys.: Condens. Matter 16 2003

(http://iopscience.iop.org/0953-8984/16/12/009)

INSTITUTE OF PHYSICS PUBLISHING JOURNAL OF PHYSICS: CONDENSED MATTER

J. Phys.: Condens. Matter **16** (2004) 2003–2016 PII: S0953-8984(04)71059-0

Numerical simulation of the defect density influence on the steady state response of a silicon-based p–i–n cell

A M Meftah[1], **A F Meftah, F Hiouani and A Merazga**

Laboratoire des Matériaux Semiconducteurs and Métalliques, Université Mohammed Khieder, BP 145, Biskra 07000, Algeria

E-mail: amjad_meftah@yahoo.fr

Received 24 October 2003
Published 12 March 2004
Online at stacks.iop.org/JPhysCM/16/2003 (DOI: 10.1088/0953-8984/16/12/009)

Abstract

This paper is concerned with the numerical simulation of the defect density influence on the steady state response of a silicon-based p–i–n cell under reverse bias dark conditions. To show this effect, the numerical simulation is performed on a crystalline cell containing a single discrete level of defects in the energy gap and in which the density of defects is varied. Afterwards, we extend our model to a typical amorphous silicon cell by including band tails and dangling bonds. The density of dangling bonds is calculated according to the defect pool model. For both cases, a detailed description of the physical model and its mathematical formulation is presented. By analysing the different variables which describe the electrical behaviour of the cell in the steady state such as the free carrier distributions, the carrier lifetimes and the quasi-Fermi levels, we show how the density of defects changes the semiconductor regime from lifetime to relaxation.

1. Introduction

The numerical simulation of semiconductor devices has been considered as an essential tool used to explain the electronic processes of the material and devices. This field of research has continued to develop and has become of interest both from the point of view of improving existing devices and the development of new ones. The electrical and optical properties of a semiconductor are limited by the density of defects in the bandgap (number of defects per unit volume per unit energy). These defects, which are represented by discrete levels in the energy gap of a crystalline semiconductor or by a continuous distribution including band tails and dangling bonds in the gap of an amorphous semiconductor, act as traps and recombination centres for excess carriers and are therefore an important parameter.

[1] Author to whom any correspondence should be addressed.

0953-8984/04/122003+14$30.00

In the non-equilibrium steady state, an excess of electron (or hole) density is characterized by two time constants. (a) Due to their mobility, the excess carriers move away into regions of lower density. The time constant for this process is the dielectric relaxation time τ_{diel}, defined by the relation

$$\tau_{\mathrm{diel}} = \frac{\varepsilon\varepsilon_0}{\sigma_0} \tag{1}$$

where σ_0 is the equilibrium conductivity, $\varepsilon_0 = 8.85 \times 10^{-14}$ F cm^{-1} the permittivity of free space and ε the dielectric constant. (b) The other process is recombination with carriers of the other type, characterized by the carrier lifetimes $\tau_{\mathrm{n,p}}$ of electrons or holes. This process tends to establish local thermal equilibrium. van Roosbroeck [1] introduced the distinction between 'lifetime semiconductors' characterized by carrier lifetimes exceeding the dielectric relaxation time

$$\tau_{\mathrm{n,p}} > \tau_{\mathrm{diel}} \tag{2}$$

and 'relaxation semiconductors', where there is a high recombination rate of electron–hole pairs leading to a short carrier lifetime:

$$\tau_{\mathrm{n,p}} < \tau_{\mathrm{diel}}. \tag{3}$$

A more exact definition can be given for the relaxation regime [2, 3]: whenever an external field is applied, there will always be a splitting of the Fermi level E_{f} into quasi-Fermi levels E_{fn} and E_{fp} for electrons and holes respectively. The magnitude of this splitting depends on the ratio $\tau_{\mathrm{diel}}/\tau_{\mathrm{n,p}}$ and on the electric field. If $\tau_{\mathrm{diel}}/\tau_{\mathrm{n,p}}$ is very small, this splitting will be rather large even for small fields. If, however, $\tau_{\mathrm{diel}}/\tau_{\mathrm{n,p}}$ is large, which is the relaxation case, the splitting is much smaller for the same field. This means that the deviations from local thermal equilibrium are negligible in the relaxation regime. As a consequence, we have

$$n(x)\,p(x) \simeq n_{\mathrm{i}}^2 \tag{4}$$

and

$$E_{\mathrm{fn}}(x) \simeq E_{\mathrm{fp}}(x) \simeq E_{\mathrm{f}}(x) \tag{5}$$

where x is the space coordinate (cm), $n(x)$ and $p(x)$ are the free electron and hole densities (cm^{-3}) at the position x and n_{i} is the intrinsic carrier density (cm^{-3}).

The aim of our work is to present a numerical simulation of the defect density effect on the electrical behaviour of a silicon p–i–n cell. We assume the dark reverse bias conditions of the steady state. We start by simulating the electrical behaviour of a crystalline cell having a single level of defects E_{r} and in which the density of defects N_{r} (cm^{-3}) is varied. Afterwards, our model is extended to a typical amorphous silicon cell by including band tail and dangling bond states.

Figure 1 shows (a) the schematic diagram of the considered p–i–n cell and (b), (c) the band diagram at thermal equilibrium for, respectively, the crystalline silicon cell and the a-Si:H one. The profile of the doping proposed in the simulation is that of an abrupt p–i–n junction.

2. Phenomenological transport equations

2.1. Crystalline silicon cell

The basic semiconductor equations forming the mathematical model, and which describe the electric transport properties within the semiconductor, are [4, 5] the Poisson equation and

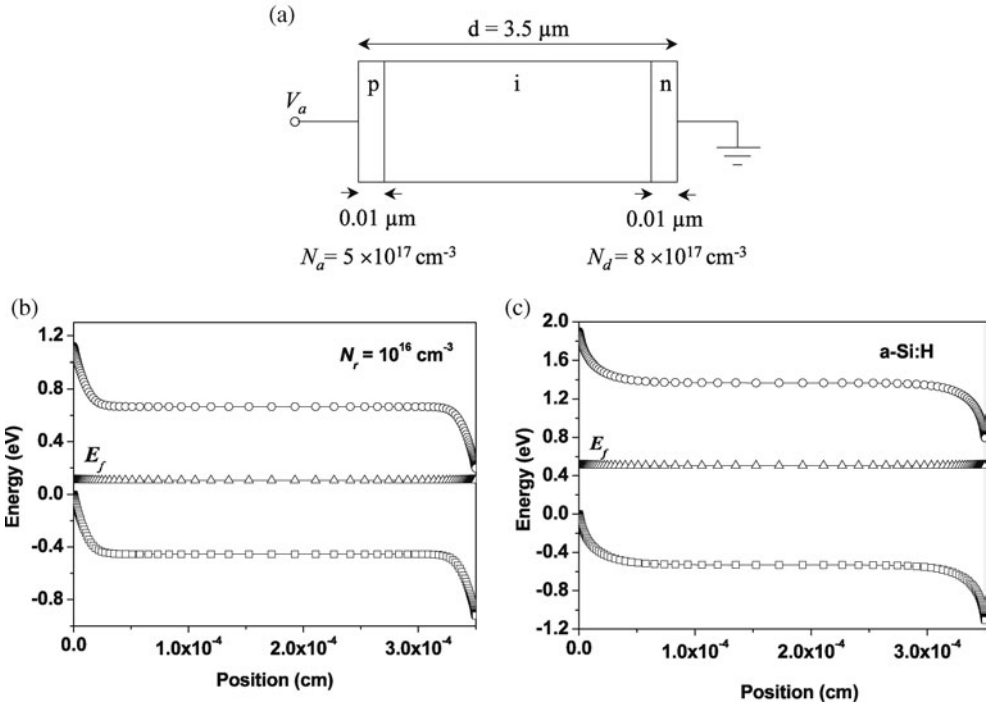

Figure 1. (a) Schematic diagram of the silicon p–i–n cell. (b), (c) Band diagram and Fermi-level profile at the thermal equilibrium of, respectively, the crystalline model with $N_\mathrm{r} = 10^{16}$ cm^{-3} and the amorphous model.

the continuity and current-density equations. In the steady state and treating the cell as a one-dimensional device, the equations can be expressed as

$$\frac{\mathrm{d}^2\psi}{\mathrm{d}x^2} = -\frac{q}{\varepsilon\varepsilon_0}\,(p - n + p_\mathrm{r} - n_\mathrm{r} + \Gamma) \tag{6}$$

$$\frac{1}{q}\frac{\mathrm{d}J_\mathrm{n}}{\mathrm{d}x} - U_\mathrm{r} = 0 \tag{7}$$

$$\frac{1}{q}\frac{\mathrm{d}J_\mathrm{p}}{\mathrm{d}x} + U_\mathrm{r} = 0 \tag{8}$$

$$J_\mathrm{n} = -q\mu_\mathrm{n} n\frac{\mathrm{d}\psi}{\mathrm{d}x} + qD_\mathrm{n}\frac{\mathrm{d}n}{\mathrm{d}x} \tag{9}$$

$$J_\mathrm{p} = -q\mu_\mathrm{p} p\frac{\mathrm{d}\psi}{\mathrm{d}x} - qD_\mathrm{p}\frac{\mathrm{d}p}{\mathrm{d}x} \tag{10}$$

where ψ is the electric potential (V), n and p are the free electron and hole densities and n_r and p_r are the trapped electron and hole densities in the discrete level E_r. J_n and J_p are the electron and hole current densities (A cm^{-2}), U_r is the recombination rate of electrons and holes (cm^{-3} s^{-1}) at the discrete level E_r, Γ is the doping charge density (cm^{-3}) and q is the elementary electric charge (C). μ_n and μ_p are the electron and hole band mobilities (cm^2 V^{-1} s^{-1}) and D_n and D_p are the electron and hole diffusion coefficients (cm^2 s^{-1}).

The trapped electron and hole densities n_r and p_r in equation (6) are, respectively, given by

$$n_\mathrm{r} = N_\mathrm{r} f_\mathrm{r} \qquad \text{and} \qquad p_\mathrm{r} = N_\mathrm{r}(1 - f_\mathrm{r}) \tag{11}$$

where N_r is the density of defects (cm^{-3}) at the level E_r and f_r is the occupation function at this level given by appendix A, in both the thermal equilibrium (equation (A.1)) and the non-equilibrium steady state (equation (A.2)).

Further, the source term U_r appearing in equations (7) and (8), which represents the recombination rate for the Shockley–Read mechanism, is given by [6]

$$U_r = \frac{np - n_i^2}{\tau_{p,r}\left(n + n_{1,r}\right) + \tau_{n,r}\left(p + p_{1,r}\right)} \tag{12}$$

where n_i is the intrinsic carrier density and $n_{1,r}$ and $p_{1,r}$ are, respectively, the effective electron and hole emission densities for the state E_r. Their expressions are given in appendix A (equation (A.3)). The characteristic times $\tau_{n,r}$ and $\tau_{p,r}$ are the carrier lifetimes for electrons and holes:

$$\tau_{n,r} = \frac{1}{C_{n,r}N_r}, \qquad \tau_{p,r} = \frac{1}{C_{p,r}N_r} \tag{13}$$

where $C_{n,r}$ and $C_{p,r}$ are the electron and hole capture coefficients ($cm^3\ s^{-1}$) for the state E_r.

2.2. Amorphous silicon cell

We now extend the previous model to the case of a typical amorphous silicon cell. This later is characterized by both band tails and dangling bonds.

The band tails result from the disorder in the atomic structure and so the absence of long range order. Therefore, we adopt the simplified exponential band tail model [7, 8], in which the conduction and valence band tail density of states ($cm^{-3}\ eV^{-1}$), as a function of the energy level E, can be expressed as

$$g_c(E) = G_c \exp\left(-\frac{E_c - E}{k_B T_c}\right) \tag{14}$$

$$g_v(E) = G_v \exp\left(-\frac{E - E_v}{k_B T_v}\right) \tag{15}$$

where k_B is the Boltzmann constant, E_c and E_v are conduction and valence band edge energies, G_c and G_v are the densities of states ($cm^{-3}\ eV^{-1}$) in E_c and E_v respectively and T_c and T_v are the characteristic absolute temperatures of the conduction and valence band tail respectively.

Besides the tail states, there are other defect states localized inside the gap which result from the presence of the dangling bonds, i.e., unsaturated broken bonds. The dangling bond states are characterized by three different charge states: D^+, D^0 and D^-, corresponding to a dangling bond occupied by zero, one and two electrons, respectively, and given by

$$D^+(E) = D(E)f^+(E), \qquad D^-(E) = D(E)f^-(E) \qquad D^0(E) = D(E)f^0(E) \tag{16}$$

where $f^+(E)$, $f^-(E)$ and $f^0(E)$ are the occupation functions in each charge state, for which expressions are given in appendix B and $D(E)$ is the dangling bond density ($cm^{-3}\ eV^{-1}$).

To calculate the density of dangling bonds, we have used the defect pool model [9–11]. According to the last version of this model developed by Powell and Deane [11], the energy variation of the dangling bond density $D(E)$ has the following expression:

$$D(E) = \gamma \left[\frac{2}{f^0(E)}\right]^{k_B T^*/2E_{vo}} P\left(E + \frac{\sigma^2}{2E_{vo}}\right) \tag{17}$$

where γ is a multiplying factor, $P(E)$ is the Gaussian distribution of the defect pool model, σ is the width of the defect pool, T^* is the equilibrium temperature (freeze-in temperature) for

which the density of states is maintained and $E_{vo} = k_B T_v$. Note that the detailed expressions of γ and $P(E)$ are given in appendix C.

Thereafter, with the inclusion of band tail states and dangling bond states, the electronic transport become more complicated in the case of amorphous silicon. Indeed, the Poisson equation (equation (6) for crystalline silicon) includes, now, the trapped charge density in both band tail states and dangling bond states:

$$\frac{d^2\psi}{dx^2} = -\frac{q}{\varepsilon\varepsilon_0}(p - n + p_t - n_t + N_{db}^+ - N_{db}^- + \Gamma). \tag{18}$$

In equation (18), the trapped electron and hole densities in the band tail states, n_t and p_t respectively, are related to the densities of states of the conduction $g_c(E)$ and valence $g_v(E)$ band tails (given by equations (14) and (15)), as

$$n_t = \int_{E_v}^{E_c} g_c(E) f_{nc}(E)\, dE \tag{19}$$

$$p_t = \int_{E_v}^{E_c} g_v(E) f_{pv}(E)\, dE \tag{20}$$

where $f_{nc}(E)$ and $f_{pv}(E)$ are, respectively, the occupation functions of electrons and holes in conduction and valence band tails given in appendix D for both thermal equilibrium (equations (D.1)) and non-equilibrium steady state (equations (D.2)).

Furthermore, the additional terms N_{db}^- and N_{db}^+ in equation (18) are the trapped electron and hole densities in the dangling bond states and are related, as in band tail states, to their respective occupation functions and density of dangling bonds as

$$N_{db}^- = \int_{E_v}^{E_c} D^-(E)\, dE \tag{21}$$

$$N_{db}^+ = \int_{E_v}^{E_c} D^+(E)\, dE \tag{22}$$

where $D^-(E)$ and $D^+(E)$ are the densities of charged states given by equation (16).

By including both band tail states and dangling bond states, the recombination rate U_r in equations (7) and (8) is replaced, in the case of amorphous silicon, by the total recombination rate, U_{tot}, which is the sum of the recombination rate U_t through band tail states and the recombination rate U_{db} through the dangling bond states.

The recombination rate U_t via band tail states is given by the following expression:

$$U_t = \int_{E_v}^{E_c} \left(np - n_i^2\right) \left\{ \left[\frac{C_{nc} C_{pc} g_c(E)}{C_{nc}(n + n_1) + C_{pc}(p + p_1)} \right] + \left[\frac{C_{nv} C_{pv} g_v(E)}{C_{nv}(n + n_1) + C_{pv}(p + p_1)} \right] \right\} dE \tag{23}$$

where C_{nc}, C_{pc}, C_{nv} and C_{pv} are the capture coefficients of electrons and holes by conduction and valence band tails respectively. n_1 and p_1 are, respectively, the effective electron and hole emission density for the state E.

The recombination rate U_{db}, through the dangling bond states, is the sum of the recombination rate U_{db}^+ via the D^+ states and U_{db}^0 via the D^0 states if we treat electrons, or the sum of the recombination rate U_{db}^- via the D^- states and U_{db}^0 via the D^0 states if we treat holes. Thus, we have

$$\begin{aligned} U_{db} &= \left(U_{db}^+ + U_{db}^0\right)_{electrons} = \left(U_{db}^- + U_{db}^0\right)_{holes} \\ &= \int_{E_v}^{E_c} \left(np - n_i^2\right) \left\{ \left[\frac{P^- C_n^+ C_p^0 + N^+ C_n^0 C_p^-}{N^+ P^- + P^0 P^- + N^+ N^0} \right] D(E) \right\} dE \end{aligned} \tag{24}$$

Table 1. Electrical parameters of the crystalline silicon cell.

Fixed parameters	
$k_B T/q = 25.87$ V	$E_g = 1.12$ eV
$\varepsilon\varepsilon_0 = 1.0625 \times 10^{-12}$ F cm^{-1}	$n_i = 10^{10}$ cm^{-3}
$T = 300$ K	$E_c - E_r = 0.56$ eV
$\mu_n = 1350$ cm^2 V^{-1} s^{-1}	$n_{1,r} = p_{1,r} = 10^{10}$ cm^{-3}
$\mu_p = 480$ cm^2 V^{-1} s^{-1}	$C_{n,r} = C_{p,r} = 10^{-8}$ cm^3 s^{-1}
$D_{n,p} = \mu_{n,p} k_B T/q$	
Variable parameters	
$N_r = 10^{12}$, 10^{14}, 10^{15}, and 10^{16} cm^{-3}	

Table 2. Electrical parameters of the a-Si:H cell.

$\varepsilon\varepsilon_0 = 1.0536 \times 10^{-12}$ F cm^{-1}	$E_g = 1.9$ eV
$T = 300$ K	$G_c = G_v = 2 \times 10^{21}$ cm^{-3} eV^{-1}
$\mu_n = 10$ cm^2 V^{-1} s^{-1}	$T = 300$ K
$\mu_p = 1$ cm^2 V^{-1} s^{-1}	$T_c = 250$ K
$D_{n,p} = \mu_{n,p} k_B T/q$	$T_v = 550$ K
$H = 5 \times 10^{21}$ cm^{-3}	$C_{nc} = C_{pv} = 10^{-8}$ cm^3 s^{-1}
$N_{SiSi} = 2 \times 10^{23}$ cm^{-3}	$C_{nv} = C_{pc} = 10^{-10}$ cm^3 s^{-1}
$E_p = 1.27$ eV	$C_n^+ = C_p^- = 10^{-7}$ cm^3 s^{-1}
$\sigma = 0.178$ eV	$C_n^0 = C_p^0 = 10^{-8}$ cm^3 s^{-1}
$T^* = 500$ K	$U = 0.2$ eV

where

$$P^0 = n_1^+ C_n^+ + p C_p^0 \tag{25a}$$

$$P^- = n_1^0 C_n^0 + p C_p^- \tag{25b}$$

$$N^0 = n C_n^0 + p_1^- C_p^- \tag{25c}$$

$$N^+ = n C_n^+ + p_1^0 C_p^0. \tag{25d}$$

In the expressions above, C_n^+, C_n^0, C_p^0 and C_p^- are electron and hole capture coefficients by D^+, D^0 and D^-, respectively. The terms n_1^0 and n_1^+ indicate, respectively, the emission of an electron to the conduction band from the D^- defect state and the D^0 defect state [12],

$$n_1^0(E) = 2N_c \exp\left(-\frac{E_c - E - U}{k_B T}\right) \qquad \text{and} \qquad n_1^+(E) = 0.5N_c \exp\left(-\frac{E_c - E}{k_B T}\right) \tag{26}$$

while the terms p_1^0 and p_1^- indicate, respectively, the emission of a hole to the valence band from the D^+ defect state and the D^0 defect state [12]:

$$p_1^0(E) = 2N_v \exp\left(-\frac{E - E_v}{k_B T}\right) \qquad \text{and} \qquad p_1^-(E) = 0.5N_v \exp\left(-\frac{E + U - E_v}{k_B T}\right). \tag{27}$$

U is the energy difference between the two-electron D^- energy state and the one-electron D^0 energy state.

3. Semiconductor parameters

Tables 1 and 2 give the electrical parameters used in the simulation of the crystalline and the amorphous silicon cell respectively. Values of the dangling bond density parameters are

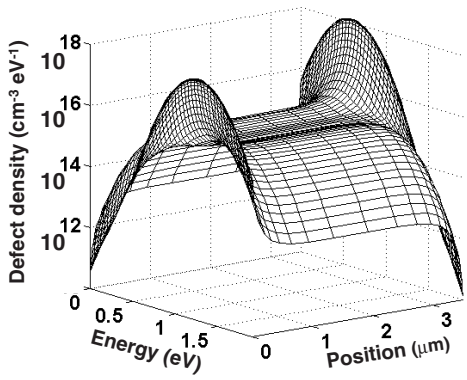

Figure 2. Spatial and energetic variation of the dangling bond density calculated by the defect pool model.

typical values found in the literature [11]. For both cases, the total device thickness d is equal to 3.5 μm; the p- and n-layer thicknesses are equal to 0.01 μm with doping densities $N_a = 5 \times 10^{17}$ cm^{-3} and $N_d = 8 \times 10^{17}$ cm^{-3} respectively.

Because the band diagram of the cell vary with space, there will be a spatial variation of the Fermi-level position within the energy 'gap'. According to the defect pool model, the dangling bond density is related to the Fermi-level position; then, there will be, in addition to the energetic variation, a spatial variation of the dangling bond density. Figure 2 shows the spatial and energetic variation of the dangling bond density calculated by the defect pool model with the parameters listed in table 2. At the p side of the cell, most of the dangling bonds are in the D^+ states. In the intrinsic layer, the Fermi level is almost in the middle of the energy 'gap', so the defect density distribution is symmetric about the D^0 peak. Going towards the n side, the dangling bonds become, more and more, in the D^- states.

4. Boundary conditions

For both crystalline and amorphous cells, boundary conditions for free carrier densities (n, p) are those of the thermal equilibrium in the p and n layers. Concerning the electric potential, the values at the boundaries $x = 0$ and d are, respectively, equal to the externally applied voltage V_a and the junction built-in potential V_i: $\psi(0) = V_a$ and $\psi(d) = V_i$.

5. Numerical method of resolution

The system defined by the basic semiconductor equations, for both crystalline and amorphous cells, cannot be solved analytically. The problem must be approached numerically. When solving the semiconductor equations, the potential ψ and the free carrier densities n and p are used as the independent variables. But before the numerical resolution, it is necessary to discretize the device into a number of slices. We have chosen a non-uniform slice distribution to show, more clearly, the variation of the different variables at the p/i and i/n interfaces. The number of spatial slices, L, is taken equal to 150. For the a-Si:H cell, the energy 'gap', in each slice, is also discretized into a number N of energy slices; N is taken equal to 50. After the discretization, the differential operators in the equations are replaced at each of the mesh points by finite difference equations where only the nearest neighbouring points are taken into account. The obtained system is a set of $3 \times L$ non-linear algebraic equations with $3 \times L$ unknowns (n, p and ψ in each slice). Generally, iterative methods are used to solve systems

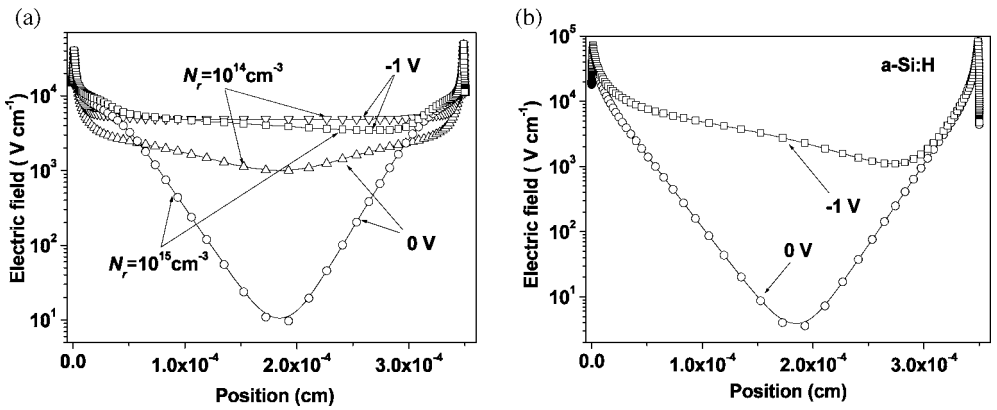

Figure 3. Electric field distribution under 0 and −1 V bias in (a) the crystalline silicon cell for two densities of defects $N_r = 10^{14}$ and 10^{15} cm^{-3}, (b) field profile in the a-Si:H cell.

of non-linear algebraic equations. The method that we have used is the iterative method of Newton [4, 5]; this one is a fully coupled method which consists of solving simultaneously the set of $3 \times L$ equations.

6. Results

Figure 3 shows the electric field distribution in the crystalline cell (case (a)) and the amorphous one (case (b)) under 0 and −1 V reverse bias voltage in the dark. For the crystalline cell, the field is plotted for two values of the defect density: 10^{14} and 10^{15} cm^{-3}. The two cases of the figure show an increase of the field from the boundaries ($x = 0$ and d) towards the p/i and i/n interfaces, followed by a decrease from the two interfaces towards the middle part of the device. The effect of defects is clearest at the thermal equilibrium. We can see that the increase of the defect density (from 10^{14} cm^{-3} to the a-Si:H density) leads to a more important decrease with an exponential decay towards the middle of the device. Under a reverse applied voltage, the depletion regions, for the two cases ((a) and (b)), are extended from both sides of the device (p and n) towards the central part until they overlap and the field increases mainly in the intrinsic layer. At the p/i and i/n interfaces, no supplementary increase is remarked for the field because the carriers here are already depleted.

Figure 4 shows the free electron and hole distributions under 0 and −1 V reverse bias voltage, always in the dark. Cases (a)–(d) correspond, respectively, to a defect density of 10^{12}, 10^{14}, 10^{15} and 10^{16} cm^{-3} in the crystalline cell. Case (e) corresponds to the a-Si:H cell. By comparing the carrier distributions under the reverse bias to those of the thermal equilibrium for each case, we remark that the −1 V voltage causes a considerable depletion of the free carriers only for $N_r = 10^{12}$ and 10^{14} cm^{-3} (cases (a) and (b)). A higher density of defects reduces the effect of the applied voltage and there is no significant deviation from the thermal equilibrium. For $N_r = 10^{16}$ cm^{-3} (case (d)), the free carrier densities under the reverse bias are almost superposed on those of the thermal equilibrium. For the a-Si:H cell, it is shown that the slight decrease of the electron density under the reverse bias (relatively to the thermal equilibrium density) is opposed by a slight increase of the hole density to maintain the thermal equilibrium condition $np = n_i^2$.

To show this effect more clearly, we have plotted in figure 5 the $n(x)p(x)$ product profile under −1 V reverse voltage for each case of figure 4. As shown, the increase of

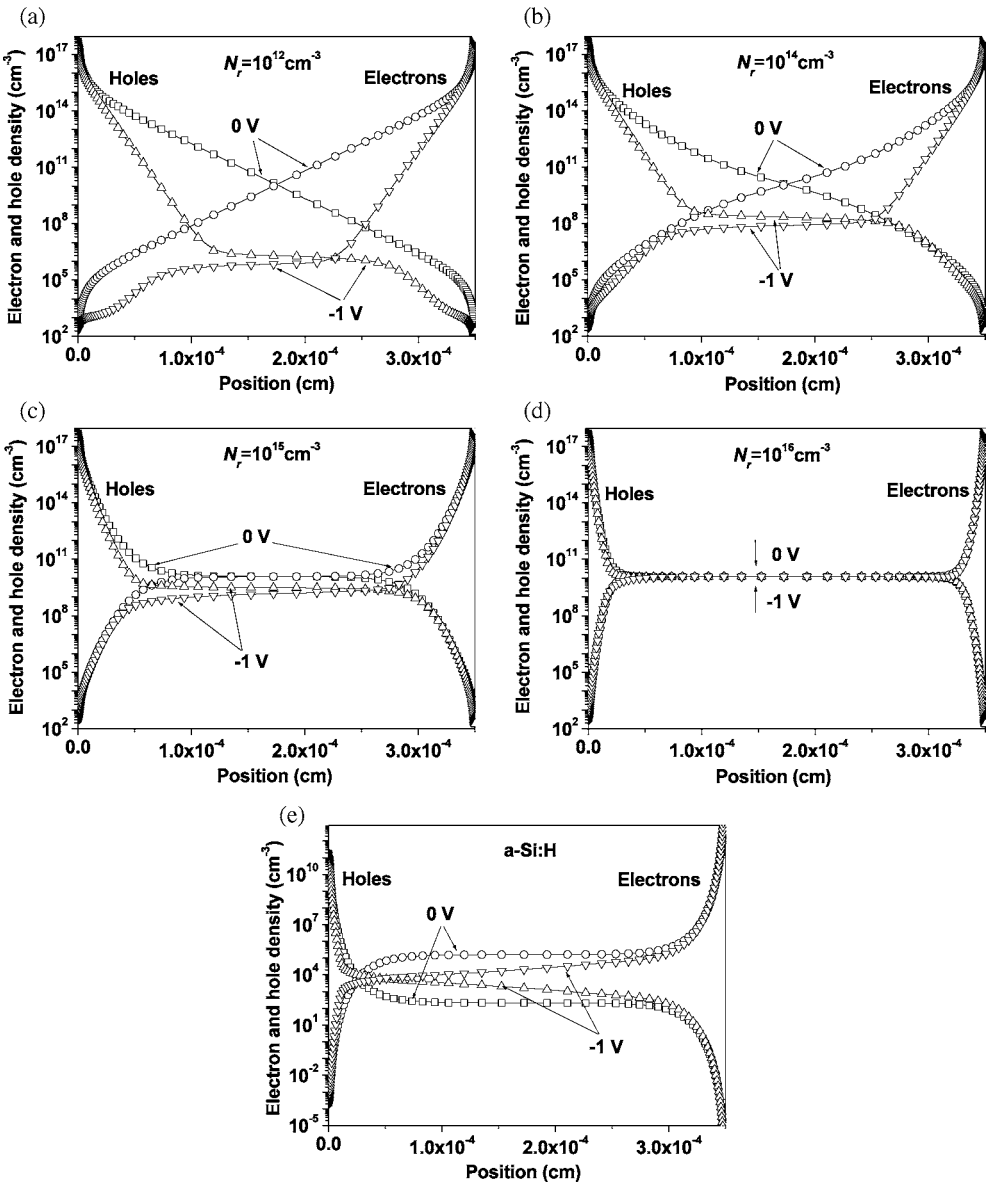

Figure 4. Free electron and hole distributions under 0 and −1 V bias in the crystalline silicon cell for different densities of defects, (a) $N_r = 10^{12}$ cm^{-3}, (b) $N_r = 10^{14}$ cm^{-3}, (c) $N_r = 10^{15}$ cm^{-3} and (d) $N_r = 10^{16}$ cm^{-3}. (e) Free electron and hole distributions in the a-Si:H cell.

the defect density reduces the effect of the applied voltage remarkably and the known relation $np = n_i^2 \exp(eV_a/k_BT)$ is no longer verified. For the crystalline case with $N_r = 10^{16}$ cm^{-3} or the amorphous case, there is almost no deviation from the thermal equilibrium; we have $n(x)p(x) \simeq n_i^2$ for all x. Even if we increase the reverse voltage to −5 or −10 V as shown in figure 6 for the two last cases, the deviation from thermal equilibrium remains very slight relative to the values of the applied voltage.

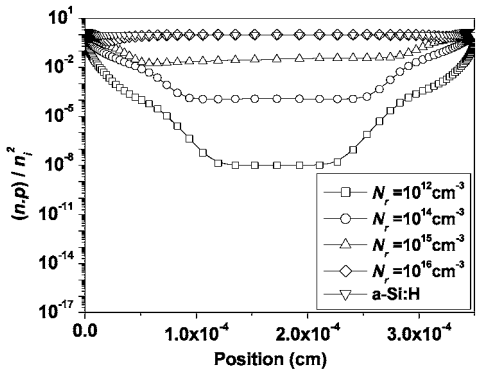

Figure 5. $n(x)\,p(x)$ product profile under -1 V bias in the crystalline silicon cell for different densities of defects and in the a-Si:H cell.

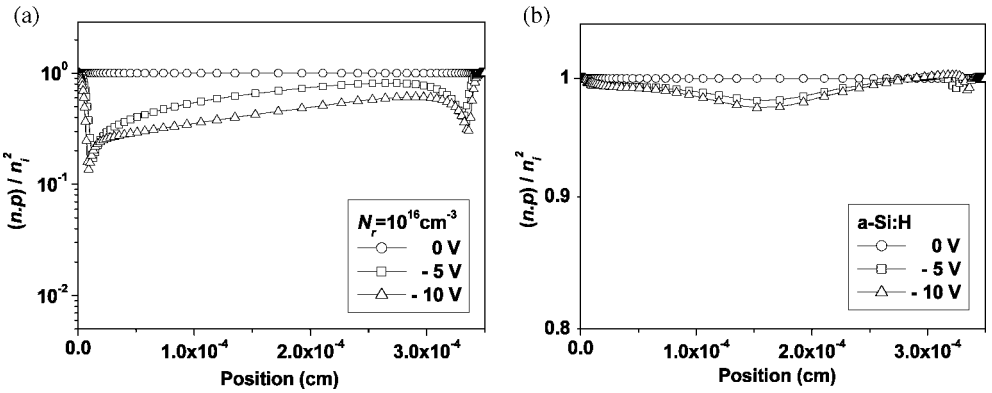

Figure 6. $n(x)\,p(x)$ product profile under 0, -5 and -10 V in (a) the crystalline silicon cell for $N_{\mathrm{r}} = 10^{16}$ cm^{-3} and (b) the a-Si:H cell.

This condition which has appeared with increasing defect density defines the relaxation regime of the semiconductor. This regime, as we mentioned in the introduction, is reached when the relaxation time is greater than the carrier lifetimes (relation (3)). Then, the increase of the defect density has changed the regime of the semiconductor from the lifetime regime to the relaxation one. We can verify this by comparing the relaxation time with the carrier lifetimes for different densities of defects. Figure 7 shows the distribution of the relaxation time $\tau_{\mathrm{diel}}(x)$ and the carrier lifetimes $\tau_{\mathrm{n}}(x)$ and $\tau_{\mathrm{p}}(x)$ through the device. For the crystalline cell, the curves are plotted for $N_{\mathrm{r}} = 10^{14}$, 10^{15} and 10^{16} cm^{-3}. $\tau_{\mathrm{diel}}(x)$ is calculated according to the relation

$$\tau_{\mathrm{diel}}(x) = \frac{\varepsilon\varepsilon_0}{\sigma_0(x)} = \frac{\varepsilon\varepsilon_0}{e\left(\mu_{\mathrm{n}} n_0(x) + \mu_{\mathrm{p}} p_0(x)\right)} \tag{28}$$

where $n_0(x)$ and $p_0(x)$ are the free electron and hole distributions at the thermal equilibrium.

For the crystalline cell, the density of defects is taken equal to the same value along the whole structure; then $\tau_{\mathrm{n}}(x)$ and $\tau_{\mathrm{p}}(x)$ will have a fixed value. By assuming the same coefficient of capture for the electrons and holes (see table 1) we have

$$\tau_{\mathrm{n}}(x) = \tau_{\mathrm{p}}(x) = \frac{1}{C_{\mathrm{n,r}} N_{\mathrm{r}}}. \tag{29}$$

For the amorphous silicon cell, the carrier lifetimes are limited by recombination of carriers via the dangling bond states, the electrons in the D^+ states and the holes in the D^- states. As

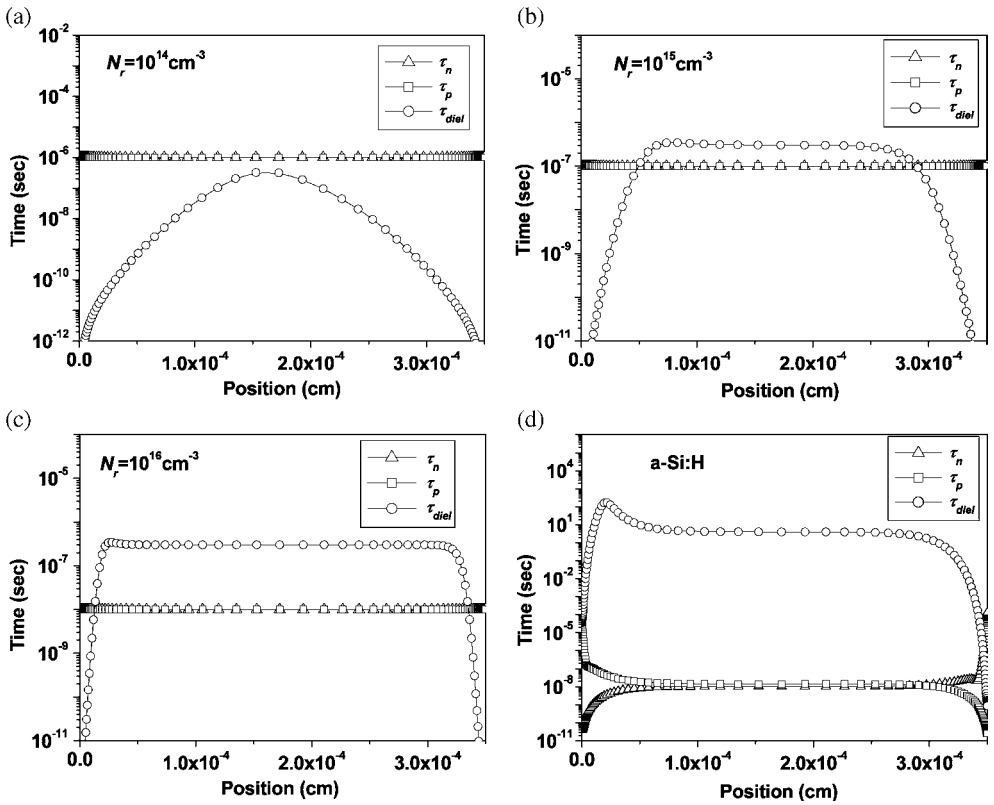

Figure 7. Relaxation time and carrier lifetime profiles in the crystalline silicon cell for (a) $N_r = 10^{14}$ cm^{-3}, (b) $N_r = 10^{15}$ cm^{-3} and (c) $N_r = 10^{16}$ cm^{-3}. (d) Relaxation time and carrier lifetime profiles in the a-Si:H cell.

these states and also their occupation functions have a spatial and energetic distribution, then the carrier lifetimes will have a spatial distribution. If $D(E, x)$ is the density of dangling bonds at the level E and in the position x, with $f^+(E, x)$ and $f^-(E, x)$ its occupation functions, then we have

$$\tau_n(x) = \left(\int_{E_v}^{E_c} C_n^+ D(E, x) f^+(E, x)\, dE \right)^{-1} \tag{30}$$

$$\tau_p(x) = \left(\int_{E_v}^{E_c} C_p^- D(E, x) f^-(E, x)\, dE \right)^{-1}. \tag{31}$$

According to figure 7, the condition of the relaxation regime is well verified on a big part of the crystalline cell for $N_r = 10^{15}$ and 10^{16} cm^{-3}, and also for the amorphous silicon cell in, which the relaxation time is greater than the carrier lifetimes by many orders of magnitude.

We can also show the transition from the lifetime regime to the relaxation one by tracing the quasi-Fermi levels under reverse bias as shown in figure 8. According to this figure, the splitting of the Fermi level $E_f(x)$ into quasi-Fermi levels $E_{fn}(x)$ (for electrons) and $E_{fp}(x)$ (for holes) under -1 V reverse voltage becomes smaller and smaller throughout the device with increasing defect density. For the two last cases ((c) and (d)), we can see that the quasi-Fermi levels are well superposed along the whole structure which means that the deviations from local thermal equilibrium are negligible.

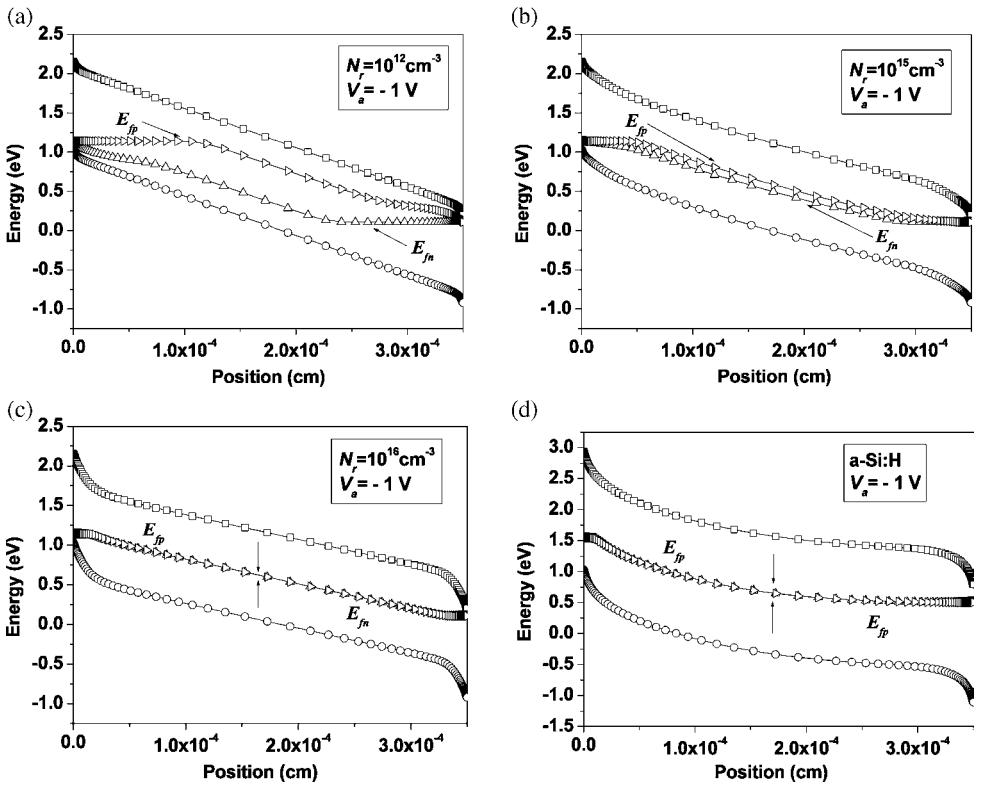

Figure 8. Bandgap and quasi-Fermi level distribution under −1 V bias in the crystalline silicon cell for (a) $N_r = 10^{12}$ cm^{-3}, (b) $N_r = 10^{15}$ cm^{-3} and (c) $N_r = 10^{16}$ cm^{-3}. (d) Bandgap and quasi-Fermi level distribution in the a-Si:H cell.

7. Conclusion

We have presented a numerical simulation of the defect density effect on the steady state electrical behaviour of a silicon-based p–i–n cell under reverse bias dark conditions. The simulation was performed on a crystalline cell having a single discrete level of defects in the energy gap and in which the density of defects is varied. Afterwards, the discrete level was replaced by a continuous distribution along the gap including band tail and dangling bond states to represent a typical amorphous silicon cell. The density of dangling bonds was calculated by the defect pool model. For both cases, a detailed description of the physical model and its mathematical formulation was presented. We have analysed, from the crystalline to the a-Si:H cell, the different variables which describe the electrical behaviour of the cell in the steady state such as the electric field profiles, the free carrier distributions, the carrier lifetimes and the quasi-Fermi levels. We have, thus, shown how the density of defects leads to a change of the semiconductor regime from a lifetime semiconductor to a relaxation one.

Appendix A

For the crystalline silicon, the occupation function f_r, in the thermal equilibrium at the discrete level E_r, is simply that of Fermi and Dirac [5, 13]:

$$f_r = \frac{1}{1 + \exp\left(\frac{E_r - E_f}{k_B T}\right)} \tag{A.1}$$

where k_B is the Boltzmann constant, T is the absolute temperature and E_f is the Fermi level at thermal equilibrium.

In the non-equilibrium steady state, the occupation function at the level E_r is one calculated by the statistic of Taylor and Simmons applied to the Shockley–Read–Hall model [6] and is given by

$$f_r = \frac{C_{n,r}n + C_{p,r}p_{1,r}}{C_{n,r}n + C_{p,r}p + C_{n,r}n_{1,r} + C_{p,r}p_{1,r}} \tag{A.2}$$

where $C_{n,r}$ and $C_{p,r}$ are the electron and hole capture coefficients ($cm^3\ s^{-1}$) for the state E_r, and

$$n_{1,r} = n_i \exp\left(\frac{E_r - E_{fi}}{k_B T}\right) \qquad \text{and} \qquad p_{1,r} = n_i \exp\left(-\frac{E_r - E_{fi}}{k_B T}\right) \tag{A.3}$$

in which n_i is the intrinsic carrier density and E_{fi} is the intrinsic Fermi level. In our case, we have taken $E_r = E_{fi}$, and then $n_{1,r} = p_{1,r} = n_i$.

Appendix B

The occupation functions f^+, f^0 and f^- of the dangling bond in each charge state, i.e., occupied, respectively, by zero, one and two electrons, are calculated at the thermal equilibrium from statistical mechanics [14] and are given by

$$f^+(E) = \frac{1}{1 + 2\exp([E_f - E]/k_B T) + \exp([2E_f - 2E - U]/k_B T)} \tag{B.1a}$$

$$f^0(E) = \frac{2\exp([E_f - E]/k_B T)}{1 + 2\exp([E_f - E]/k_B T) + \exp([2E_f - 2E - U]/k_B T)} \tag{B.1b}$$

$$f^-(E) = \frac{\exp([2E_f - 2E - U]/k_B T)}{1 + 2\exp([E_f - E]/k_B T) + \exp([2E_f - 2E - U]/k_B T)} \tag{B.1c}$$

where U is the correlation energy which is the energy difference between the two-electron D^- energy state and the one-electron D^0 energy state.

In the non-equilibrium steady state, the occupation functions for each charge state, D^+, D^- and D^0, are expressed as [15]

$$f^+(E) = \frac{P^0 P^-}{N^+ P^- + P^0 P^- + N^0 N^+} \tag{B.2a}$$

$$f^-(E) = \frac{N^0 N^+}{N^+ P^- + P^0 P^- + N^0 N^+} \tag{B.2b}$$

$$f^0(E) = \frac{N^+ P^-}{N^+ P^- + P^0 P^- + N^0 N^+}. \tag{B.2c}$$

The expressions of P^0, P^-, N^0 and N^+ are given in section 2.2 (equations (25)).

Appendix C

In equation (17), the multiplying factor γ and the Gaussian distribution of the defect pool model $P(E)$ are given by [11]

$$\gamma = \left[\frac{G_v 2E_{vo}^2}{[2E_{vo} - k_B T^*]}\right]\left[\frac{H}{N_{SiSi}}\right]^{k_B T^*/4E_{vo}} \exp\left[\frac{-1}{2E_{vo}}\left[E_p - E_v - \frac{\sigma^2}{4E_{vo}}\right]\right] \tag{C.1}$$

$$P(E) = \left(1/\sigma\sqrt{2\pi}\right)\exp\left[-\frac{(E - E_p)^2}{2\sigma^2}\right] \tag{C.2}$$

where E_p is the most probable energy, E_v is the valence band edge energy and H and N_{SiSi} are, respectively, the total density (cm^{-3}) of hydrogen and the number of electrons in the silicon bonding states.

Appendix D

In thermal equilibrium, the occupation function of electrons $f_{nc}(E)$ in the conduction band tail is the Fermi–Dirac function:

$$f_{nc}(E) = \frac{1}{1 + \exp\left(\frac{E - E_f}{k_B T}\right)}. \tag{D.1a}$$

Likewise, for holes in the valence band tail, we have

$$f_{pv}(E) = \frac{1}{1 + \exp\left(\frac{E_f - E}{k_B T}\right)}. \tag{D.1b}$$

In the non-equilibrium steady state, the occupation functions of electrons and holes in conduction and valence band tails were determined using the Taylor–Simmons statistics and are shown to be given by [6]

$$f_{nc}(E) = \frac{C_{nc} n + C_{pc} p_1}{C_{nc} n + C_{pc} p + C_{nc} n_1 + C_{pc} p_1} \tag{D.2a}$$

$$f_{pv}(E) = \frac{C_{pv} p + C_{nv} n_1}{C_{pv} p + C_{nv} n + C_{pv} p_1 + C_{nv} n_1} \tag{D.2b}$$

where

$$n_1(E) = n_i \exp\left(\frac{E - E_{fi}}{k_B T}\right) \qquad \text{and} \qquad p_1(E) = n_i \exp\left(-\frac{E - E_{fi}}{k_B T}\right). \tag{D.3}$$

References

[1] van Roosbroeck W and Casey H C 1972 *Phys. Rev.* B **5** 2154
[2] Döhler G H and Heyszenau H 1975 *Phys. Rev.* B **12** 641
[3] Queisser H J 1972 *Solid State Dev.* **8** 145
[4] Kurata M 1982 *Numerical Analysis for Semiconductor Devices* (Lexington, MA: Heath)
[5] Selberherr S 1984 *Analysis and Simulation of Semiconductor Devices* (Berlin: Springer)
[6] Simmons J G and Taylor G W 1971 *Phys. Rev.* B **4** 502
[7] Cohen M H, Fritzsche H and Ovshinsky S R 1969 *Phys. Rev. Lett.* **22** 1065
[8] Mott N F 1970 *Phil. Mag.* **22** 7
[9] Winer K 1989 *Phys. Rev. Lett.* **63** 1487
[10] Powell M J and Deane S C 1993 *Phys. Rev.* B **48** 10815
[11] Powell M J and Deane S C 1996 *Phys. Rev.* B **53** 10121
[12] Halpern V 1986 *Phil. Mag.* B **54** 473
[13] Sze S M 1969 *Physics of Semiconductor Devices* (New York: Wiley–Interscience)
[14] Okamoto H and Hamakawa Y 1977 *Solid State Commun.* **24** 23
[15] Okamoto H, Kida H and Hamakawa Y 1984 *Phil. Mag.* B **49** 231